Available online at www.sciencedirect.com
SCIENCE DIRECT
Journal of Crystal Growth 289 (2006) 686–689
JOURNAL OF CRYSTAL GROWTH
www.elsevier.com/locate/jcrysgro

Growth of In_2O_3 single-crystalline film on sapphire (0 0 0 1) substrate by molecular beam epitaxy

Z.X. Mei[a,*], Y. Wang[a], X.L. Du[a], Z.Q. Zeng[a], M.J. Ying[a], H. Zheng[a], J.F. Jia[a], Q.K. Xue[a,*], Z. Zhang[b]

[a]*Institute of Physics, Chinese Academy of Sciences, Beijing 100080, China*
[b]*Beijing University of Technology, Beijing 100022, China*

Received 11 October 2005; received in revised form 28 November 2005; accepted 1 December 2005
Available online 10 February 2006
Communicated by M. Kawasaki

Abstract

In_2O_3 (1 1 1) single-crystalline films have been grown on sapphire (0 0 0 1) substrate by RF plasma-assisted molecular beam epitaxy. The epitaxial relationship between the film and substrate was determined by in situ reflection high-energy electron diffraction, ex situ X-ray diffraction and transmission electron microscopy. Optical and electrical measurements show that the undoped In_2O_3 films are highly transparent and conductive. Twin crystals were observed as the main defects in the film by high-resolution electron microscopy. The film may be used for transparent electrical contact in optoelectronic devices, such as ZnO-based ultraviolet diodes and lasers.

PACS: 81.15.Hi; 68.55.−a

Keywords: A1. Reflection high-energy electron diffraction; A1. Sapphire (0 0 0 1) substrate; A1. Twin crystal; A3. Molecular beam epitaxy; B2. In_2O_3; B2. Transparent conductive oxide

In_2O_3 is a wide band gap (~3.7 eV) semiconductor with optical transmittance in excess of 80% within the visible spectral region [1,2]. Stoichiometric In_2O_3 single crystal shows high resistivity (ρ) (greater than $10^4\,\Omega$ cm) [3]. However, it can become highly conductive ($\rho \sim 10^{-4}\,\Omega$ cm) by doping with valence cations such as Sn [4]. Oxygen vacancies are another sources of conducting electrons, accounting for the low resistivities observed in undoped, oxygen deficient materials [5]. In_2O_3 crystallizes in cubic bixbyite structure with the space group of Ia3, and its complicated unit cell contains 80 atoms with a lattice parameter of 10.118 Å, in which the 32 In^{3+} ions occupy the 8b and 24d sites and the 48 O^{2-} occupy the 48f site, respectively. The 16c site is the quasi-anion site unoccupied, whose regular arrangement leads to a superstructure in In_2O_3 single crystal [6].

A wide range of device applications and fundamental research [7–10] need transparent conductive oxide (TCO) materials with wide band gaps such as In_2O_3, ZnO, and SnO_2, etc. They are especially desirable for thin film optoelectronic devices [11–14]. TCOs are necessary either to raise the work functions for Schottky contacts in metal–semiconductor–metal (MSM) photodiodes or to lower the contact resistance for ohmic contacts in photoswitching devices. The well-known transparent tin-doped indium oxide (ITO) has been suggested due to its potent nature of ohmic or Schottky contacts, as observed in n-GaN films [15,16]. ITO films may be more promising for such applications in ZnO-based devices mainly due to its high stability in their coherent oxide growth process. However, very few studies on ITO/ZnO contact have been reported. The complex nature of polycrystalline In_2O_3 films and the large number of processing parameters have hampered the progress.

For single-crystalline In_2O_3 film growth, MgO and yttria-stabilized zirconia (YSZ) were adopted as substrates

*Corresponding authors.
E-mail addresses: zxmei@aphy.iphy.ac.cn (Z.X. Mei), qkxue@aphy.iphy.ac.cn (Q.K. Xue).

0022-0248/$ - see front matter © 2006 Elsevier B.V. All rights reserved.
doi:10.1016/j.jcrysgro.2005.12.086

[17–19]. However, there is no report on the growth of In_2O_3 film on α-Al_2O_3 (0 0 0 1) substrate, which is readily available with high quality and widely used in ZnO heteroepitaxy [20,21].

In this work, we have investigated the growth of In_2O_3 (1 1 1) films on sapphire (0 0 0 1) substrate by an RF plasma-assisted MBE system (MBE-IV, ShenYang KeYi). The choice of MBE enables the complicated growth parameters more precisely controlled. The crystal structures were studied in situ by reflection high-energy electron diffraction (RHEED) and ex situ by an X-ray diffractometer (XRD) (Dede D1) and a Philips CM200 field emission transmission electron microscope operating at 200 KV, respectively. The base pressure in the growth chamber was $\sim 5 \times 10^{-10}$ Torr. High-purity In metal (99.9999%) was evaporated from a commercial Knudsen cell. Active oxygen radicals were produced by passing high-purity oxygen gas (99.999%) through an RF-plasma system (HD25R, Oxford Applied Research).

After degreased in trichloroethylene and acetone, the sapphire substrate was chemically etched in a hot solution of H_2SO_4:H_3PO_4 = 3:1 at 110 °C for 30 min and then rinsed with deionized water. Before growth, the substrate was thermally cleaned at 720 °C for 30 min, followed by oxygen radicals pretreatment at 500 °C for 30 min. Then, In_2O_3 buffer layer was grown at substrate temperature of 600 °C prior to the deposition of In_2O_3 epilayer at 680 °C.

We first discuss the detailed growth processes of the In_2O_3 films based on in situ RHEED observation. A sharp streaky pattern of the sapphire substrate was observed after oxygen radical exposure [Fig. 1(a)]. After In_2O_3 deposition at 600 °C for a few minutes, diffuse streaky patterns [Fig. 1(b)] superimposed on that of sapphire substrate appear. The sixfold symmetry and rod spacing indicate that cubic In_2O_3 grows with (1 1 1) orientation, while the streaky patterns suggest a 2D nucleation at the initial growth stage. Since the RHEED pattern of α-Al_2O_3 (0 0 0 1) substrate is still visible at this stage, the thickness should be nearly 1 ML. Further growth of In_2O_3 led to diffuse spotty patterns, indicating the onset of 2D–3D growth caused by the large lattice mismatch (−13.2%) between In_2O_3 (1 1 1) and α-Al_2O_3 (0 0 0 1) [Fig. 1(c)]. During the In_2O_3 epilayer growth at 680 °C, there is basically no big change in the RHEED pattern (not shown).

The in-plane epitaxial orientationship between In_2O_3 (1 1 1) and α-Al_2O_3 (0 0 0 1) was determined from the RHEED patterns as $In_2O_3[1\,0\,\bar{1}] \| Al_2O_3[1\,0\,\bar{1}\,0]$ and $In_2O_3[1\,1\,\bar{2}] \| Al_2O_3[1\,1\,\bar{2}\,0]$. This corresponds to a 30° in-plane rotation of the In_2O_3 lattice with respect to the substrate, as schematically shown in Fig. 1(d). The large full and open circles indicate the oxygen atoms in sapphire and the indium atoms in In_2O_3, respectively. It can be seen that the hexagonally packed indium plane of In_2O_3 (1 1 1) is matched to the close-packed oxygen plane of sapphire with a rotation of 30° from the main lattice. This relationship is further confirmed with high-resolution electron microscopy (HREM) measurements, which will be discussed later.

Fig. 2 shows the XRD θ–2θ scan curve of the In_2O_3 film. Four peaks are observed at $2\theta = 30.5°$, 41.7°, 63.5° and 90.7° which correspond to the diffractions from In_2O_3 (2 2 2), sapphire (0 0 0 6), In_2O_3 (4 4 4) and sapphire (0 0 1 2), respectively. The above results indicate a cubic In_2O_3 single crystalline film with its [1 1 1] direction parallel to [0 0 0 1] direction of sapphire.

To confirm the epitaxial relationship between In_2O_3 (1 1 1) and α-Al_2O_3 (0 0 0 1), cross-section HREM measurements were performed. Fig. 3 shows the micrograph taken along $[1\,\bar{1}\,0\,0]_{sapphire}$. A continuous crystalline In_2O_3 film is found to be formed on the sapphire substrate

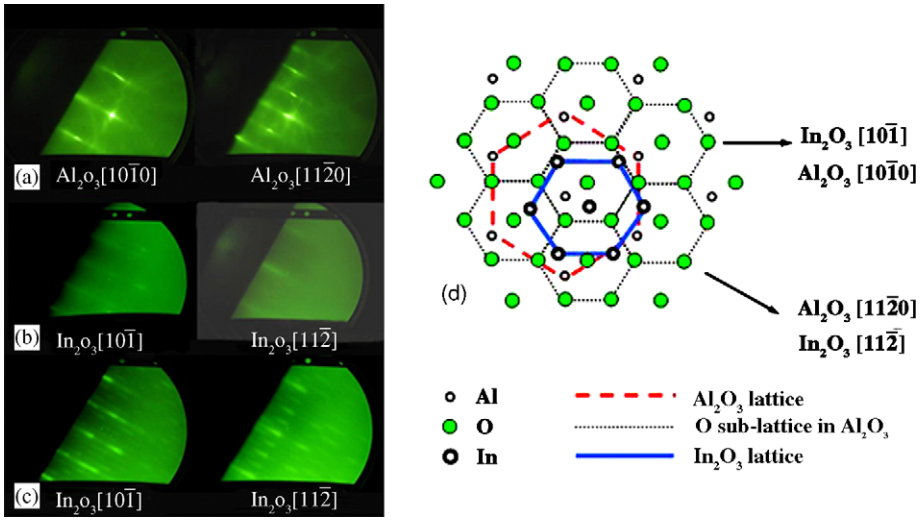

Fig. 1. RHEED patterns showing the morphology evolution during the growth of In_2O_3 film on sapphire substrate, (a) α-Al_2O_3 (0 0 0 1) surface after oxygen radical treatment, (b) In_2O_3 surface at initial 2D-nucleation stage, (c) In_2O_3 surface after 2D–3D transition. The atomic arrangement in In_2O_3 (1 1 1) and α-Al_2O_3 (0 0 0 1) planes are shown in (d).

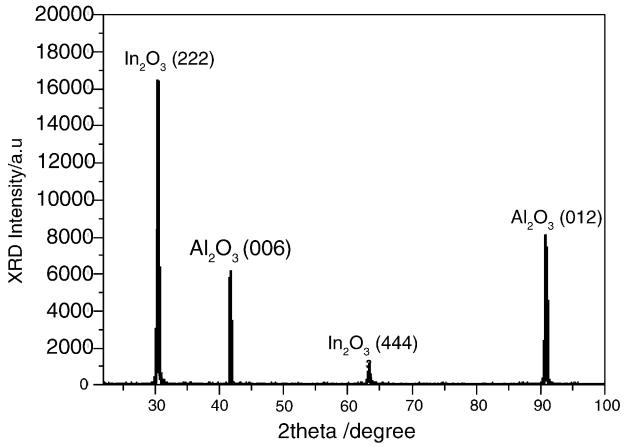

Fig. 2. XRD θ–2θ scan of the In_2O_3 film. Four peaks at $2\theta = 30.5^\circ$, 41.7°, 63.5° and 90.7° are originated from In_2O_3 (2 2 2), sapphire (0 0 0 6), In_2O_3 (4 4 4) and sapphire (0 0 1 2), respectively.

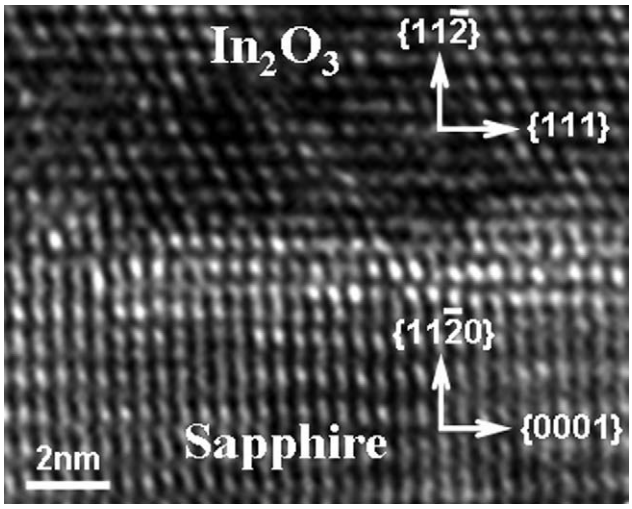

Fig. 3. HREM image taken along $[1\,\bar{1}\,0\,0]_{sapphire}$. The epitaxial relationship is $In_2O_3[1\,1\,1]\|Al_2O_3[0\,0\,0\,1]$ and $In_2O_3[1\,1\,\bar{2}]\|Al_2O_3[1\,1\,\bar{2}\,0]$.

with a sharp interface. From Fig. 3, the epitaxial relationship can be verified as $In_2O_3[1\,1\,1]\|Al_2O_3[0\,0\,0\,1]$ and $In_2O_3[1\,1\,\bar{2}]\|Al_2O_3[1\,1\,\bar{2}\,0]$, in agreement with the RHEED observation.

For a desirable TCO material, In_2O_3 must show high optical transmittance within the visible spectral region and good electrical conductivity. From optical absorption spectra of the undoped In_2O_3 films, a transmittance beyond 80% was found within the visible spectral region (not shown here). Hall measurements show resistivities in the order of $10^{-3}\,\Omega\,cm$, with a mobility of about $30\,cm^2/Vs$. Since the films were grown in oxygen-sufficient conditions, and their resistivities will be lowered down further in oxygen-deficient growth conditions, these films should be very promising for the applications in optoelectronic devices as contact material.

We also studied the microstructure of In_2O_3 films by selected area electron diffraction (SAED) and HREM. We found that twin crystals with a $\{1\,1\,\bar{2}\}$ twin plane and $\langle 111 \rangle$ slide direction are the main defects, as shown in Fig. 4. It is an SAED image taken under $g = [1\,0\,\bar{1}]_{In_2O_3}$ zone axis. The diffraction spots caused by the 180° twin crystals are clearly indexed, and agree well with the HREM observation (not shown). An alternative description of this kind of twinning is 180° rotation about the twin plane normal (twin axis). 180° twins are quite common in bcc crystals [22]. They can be formed as a result of atom diffusion during recrystallization, and can relieve strain at the interface to reduce the system energy caused by the large lattice mismatch between In_2O_3 (1 1 1) and Al_2O_3 (0 0 0 1) here.

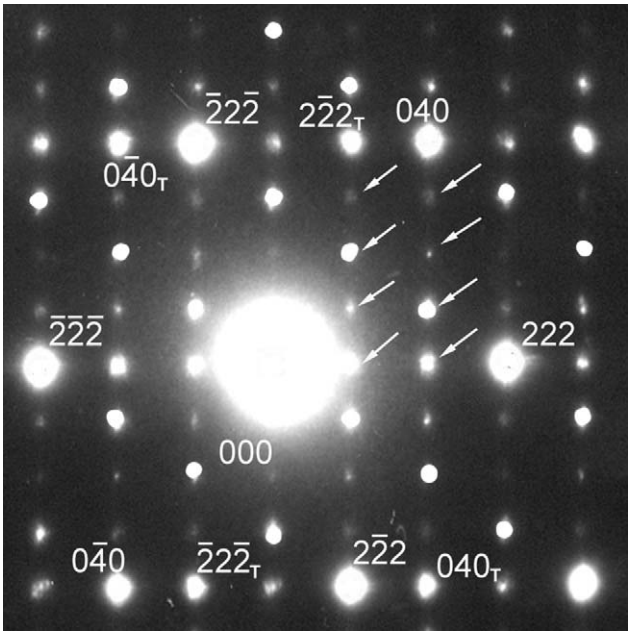

Fig. 4. SAED patterns along $g = [1\,0\,\bar{1}]_{In_2O_3}$ zone axes, where diffraction spots from twin crystals can been clearly seen. The arrowed fractional diffraction spots superimposed on the matrix may be caused by the superstructure of unoccupied quasi-anion sites in the film.

Recently, Tomita et al. suggested that interstitial indium (In_i), coexisting with oxygen vacancy (V_o), is the major point defect that accounts for the origin of the native donor in In_2O_3 [23], consistent with Rosenberg's observations [24]. Here the existence of the plane defects of 180° twin crystals in our sample may counteract the effect of the native donor by scattering the conduction electrons, but the extent of their influence on the electrical properties needs to be further investigated.

In Fig. 4, we found some unknown fractional spots (indicated by white arrows). RHEED patterns also exhibit a similar fractional structure among (0 0), (0 1) and $(0\,\bar{1})$ directions [Fig. 1(c)]. According to our speculation, the quasi-anion sites may account for the well-defined patterns. As stated above, the 16c sites are unoccupied in In_2O_3 single crystal. They align in a regular superstructure from the lattice point of view, which may introduce extra fractional diffracted spots into the matrix produced by the

cubic network of In_2O_3. Further identification of the nature of this structure is important for a clear understanding of its influence on film qualities.

In summary, single crystalline In_2O_3 (1 1 1) films have been prepared on the sapphire (0 0 0 1) substrates by RF plasma-assisted MBE, and their microstructures are characterized by XRD and HREM. The undoped films exhibit excellent optical and electrical properties, and may be used as transparent contacts for ZnO-based ultraviolet laser diodes.

This work is supported by National Science Foundation (60476044, 60376004, 60021403) and Ministry of Science and Technology (2002CB613502) of China.

References

[1] R.L. Weiher, R.P. Ley, J. Appl. Phys. 37 (1966) 299.
[2] E.B. Ali, H.E. Maliki, J.C. Bernede, M. Sahnoun, A. Khelil, O. Saadane, Mater. Chem. Phys. 73 (2002) 78.
[3] J.H.W. De Wit, J. Crystal Growth 12 (1972) 183.
[4] Y. Shigesato, S. Takaki, T. Haranoh, J. Appl. Phys. 71 (1992) 3356.
[5] J.I. Jeong, J.H. Moon, J.H. Hong, J.S. Kang, Y.P. Lee, Appl. Phys. Lett. 64 (1994) 1215.
[6] T. Omata, H. Fujiwara, S. Otsuka-Yao-Matsuo, N. Ono, Appl. Phys. A 71 (2000) 609.
[7] K.L. Chopra, S. Major, D.K. Pandya, Thin Solid Films 102 (1983) 1.
[8] I. Hamberg, C.G. Granqvist, J. Appl. Phys. 60 (1986) R123.
[9] S.B. Qadri, H. Kim, H.R. Khan, A. Pique, J.S. Horwitz, D. Chrisey, W.J. Kim, E.F. Skelton, Thin Solid Films 377–378 (2000) 750.
[10] X. Jiang, F.L. Wong, M.K. Fung, S.T. Lee, Appl. Phys. Lett. 83 (2003) 1875.
[11] M. Hagerott, H. Jeon, A.V. Nurmikko, W. Xie, D.C. Grillo, M. Kobayashi, R.L. Gunshor, Appl. Phys. Lett. 60 (1992) 2825.
[12] E. Gautier, A. Lorin, J.M. Nunzi, A. Schalchli, J.J. Benattar, D. Vital, Appl. Phys. Lett. 69 (1996) 1071.
[13] T. Margalith, O. Buchinsky, D.A. Cohen, A.C. Abare, M. Hansen, S.P. DenBaars, L.A. Coldren, Appl. Phys. Lett. 74 (1999) 3930.
[14] S.Y. Kim, H.W. Jang, J.-L. Lee, J. Vac. Sci. Technol. B 22 (2004) 1851.
[15] K.-H. Shim, M.C. Paek, B.T. Lee, C. Kim, J.Y. Kang, Appl. Phys. A 72 (2001) 471.
[16] J.K. Sheu, Y.K. Su, G.C. Chi, M.J. Jou, C.C. Liu, C.M. Chang, Solid State Electron. 43 (1999) 2081.
[17] E.J. Tarsa, J.H. English, J.S. Speck, Appl. Phys. Lett. 62 (1993) 2332.
[18] N. Taga, M. Maekawa, Y. Shigesato, I. Yasui, M. Kamei, T.E. Haynes, Jpn. J. Appl. Phys. 37 (1998) 6524.
[19] H. Ohta, M. Orita, M. Hirano, H. Hosono, J. Appl. Phys. 91 (2002) 3547.
[20] Y.F. Chen, H.-J. Ko, S.-K. Hong, T. Yao, Appl. Phys. Lett. 76 (2000) 559.
[21] Z.X. Mei, X.L. Du, Y. Wang, M.J. Ying, Z.Q. Zeng, H. Zheng, J.F. Jia, Q.K. Xue, Z. Zhang, Appl. Phys. Lett. 86 (2005) 112111.
[22] B. Fultz (Ed.), Transmission Electron Microscopy and Diffractometry of Materials, Springer, Berlin, 2001.
[23] T. Tomita, K. Yamashita, Y. Hayafuji, H. Adachi, Appl. Phys. Lett. 87 (2005) 051911.
[24] A.J. Rosenberg, J. Phys. Chem. 64 (1960) 1143.